Bayesian network-based fault detection and diagnosis of heating components in heat recovery ventilation

Wang, Ziao; Lu, Chujie; Taal, Arie; Gopalan, Srinivasan; Mohammed, Karzan; Meijer, Arjen; Itard, Laure

Publication date
2024

Document Version
Final published version

Citation (APA)
Wang, Z., Lu, C., Taal, A., Gopalan, S., Mohammed, K., Meijer, A., & Itard, L. (2024). *Bayesian network-based fault detection and diagnosis of heating components in heat recovery ventilation*. Paper presented at Roomvent 2024, Stockholm, Sweden.

Bayesian network-based fault detection and diagnosis of heating components in heat recovery ventilation

Ziao Wang[1*], *Chujie* Lu[1], *Arie* Taal[2], *Srinivasan* Gopalan[3], *Karzan* Mohammed[3], *Arjen* Meijer[1], *Laure* Itard[1]

[1]Faculty of Architecture and the Built Environment, Delft University of Technology, Delft, the Netherlands
[2]The Hague University of Applied Science, Delft, the Netherlands
[3]Department of the Built Environment, Eindhoven University of Technology, Eindhoven, the Netherlands

Abstract. This study investigates the diagnostic capabilities of a Diagnostic Bayesian Network (DBN) for air handling unit (AHU) components, particularly focusing on the heat recovery wheel (HRW) and heating coil valve (HCV). Unlike data-driven methods relying heavily on high-quality labeled data, this knowledge-based DBN is more suitable for real-world applications, where labeled faulty and normal data are hard to obtain. Notably, existing studies predominantly concentrate on developing DBN for AHU with recirculated air, neglecting thorough investigations into AHU with HRW, a prevalent system in North Europe and increasingly recommended post-COVID-19 for mitigating viral propagation. This paper presents a DBN setup with expert knowledge for an AHU with HRW, which is evaluated using experimental data from an office building in the Netherlands. The results show that the proposed DBN can successfully diagnose typical faults in HRW and HCV.

1. Introduction

In the European Union, the building sector accounts for roughly 36% of greenhouse gas emissions, and it is estimated that 75% of the building infrastructure is considered energy inefficient [1]. Heating, ventilation, and air conditioning (HVAC) systems are designed to regulate indoor temperature, maintain air quality, and control humidity for optimal occupant comfort in buildings. HVAC systems constitute a significant portion of energy use in both residential and commercial buildings, accounting for roughly half of the total energy consumption in these structures [2].

The air handling unit (AHU), as a key subsystem of HVAC systems, is responsible for introducing fresh air and removing exhaust air. It is important for maintaining energy-efficient operations and ensuring a comfortable indoor environment to detect and diagnose faults in AHU promptly and precisely [3]. Lin et al. [4] found potential energy savings from fault detection and diagnosis (FDD) of 5-30% in building energy systems. FDD methods can be divided into two main categories [5], data-driven approaches and knowledge-based approaches. Data-driven approaches can automatically capture the underlying patterns of faults from sensor data in building management systems. Many studies have applied various algorithms for FDD in AHU [6, 7], such as support vector machines [8], convolutional neural networks [9], and clustering [10]. However, pure data-driven approaches require high quality labelled faulty data for model training, which is expensive and time-consuming to obtain in practice. Besides, data-driven approaches lack interpretability and might suffer from similar data patterns caused by different faults.

Contrasting with pure data-driven approaches, knowledge-based approaches offer higher interpretability by relying on expert knowledge and diagnostic rules to discern faulty operations within systems [11]. Diagnostic Bayesian Network (DBN), as a knowledge-based approach, utilizing physical rules and probabilistic inference, offers interpretability and high accuracy for FDD in building energy systems, including AHU [12, 13], chillers [14], heat pumps [15], and so on. Notably, existing studies predominantly concentrate on developing DBN for AHU with recirculated air [13, 16]. There is a lack of investigations into developing DBN for AHU with heat recovery wheels (HRW), which is a prevalent system in North Europe and increasingly recommended post-COVID-19 for mitigating viral propagation.

To fill the research gap, this study proposes a knowledge-based DBN for FDD in heating components of AHU, especially focusing on the faults in HRW and heating coil valves (HCV). The proposed DBN follows the reference framework, four symptoms and three faults (4S3F) proposed by Taal and Itard [17]. The DBN is evaluated using experimental data from an office building in the Netherlands, one of the living laboratories within the Brain4Buildings project [18].

In the following sections, this paper will introduce the methodology, including the theory of DBN, the 4S3F framework and its implementation. Section 3 describes the case study. Subsequently, the results and discussion will be presented in Section 4. Finally,

* Corresponding author: ziao.wang@tudelft.nl

Section 5 will provide the summary and conclusion of this work.

2. Methodology

2.1 The theory of DBN

The DBN models relies on the Bayes theorem, which utilizes conditional probability to assess the likelihood of an event given the occurrence of another event. Within this framework, when considering event A, indicative of a fault, occurring in the context of event B, which represent a symptom, the probability of A given B is defined as follows:

$$P(A|B) = \frac{P(AB)}{P(B)} = \frac{P(B|A)P(A)}{P(B)} \quad (1)$$

By applying Bayes theorem, posterior probabilities can be calculated from prior probabilities. The prior probability of the variable and the conditional probability B are obtained from the existing knowledge, which may include statistical data or expert knowledge. The posterior probability is calculated as follows.

$$P(A_i|B) = \frac{P(A_i)P(B|A_i)}{\sum_{i=1}^{n} P(A_i)P(B|A_i)} \quad (2)$$

2.2 4S3F framework

Fig. 1 presents the 4S3F framework, which is a two-phase diagnostic framework, including symptom detection and fault diagnose [17, 19-21]. The initial phase utilizes data-driven analytics, expert knowledge and physical laws to identify and catalogue potential symptoms. The symptoms of the 4S3F framework in the building energy systems are divided into four types as follows.

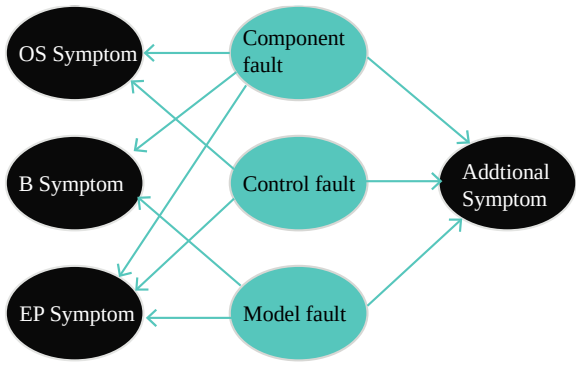

Fig. 1. The 4S3F framework for FDD in building energy systems

- "Balance symptoms" arise from energy balance discrepancies, based on quantitative models grounded in system theory and thermodynamics.
- "Energy Performance (EP) symptoms" are deviations in energy efficiency metrics.
- "Operational State (OS) symptoms" reflect variations from normal operational parameters.
- "Additional symptoms" are derived from supplementary historical and maintenance data or specific FDD processes.

The second phase involves DBN models, employing probabilistic analysis to diagnose faults based on the symptoms detected previously. The DBN models excel in HVAC fault diagnosis by calculating the likelihood of faults based on symptom occurrence, mirroring HVAC experts' diagnostic techniques. In the 4S3F framework, faults are categorized into three main types as follows.

- Component faults include malfunctions, sensor issues, or design/installation errors.
- Control faults include improper setpoints or software errors.
- Model faults include inaccurate calculations or assumptions, such as neglecting heat loss in ducts.

2.3 Implementation of 4S3F framework

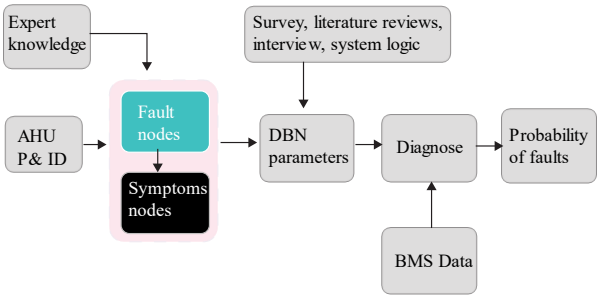

Fig. 2. The implementation of 4S3F framework

Fig. 2 depicts the implementation of 4S3F framework, which encompasses four steps, outlined as follows:

Step 1: Diagram analysis. The piping and instrumentation diagram (P&ID) of the building energy systems needs to be analysed first, including sensors, components, and control strategies, to understand the physical process and internal relationship.

Step 2: Identifying fault and symptom nodes. Based on expert knowledge and analysis, the faults and their associated symptoms need to be identified. The causal relationships between the faults and symptoms are established.

Step 3: Determining prior and conditional probabilities. Prior probabilities are the occurrence likelihood of typical faults. Conditional probabilities are the probabilities when faults are inferred based on the presence of corresponding symptoms. These probabilities can be derived from expert knowledge, maintenance records, and BMS data.

Step 4: Executing DBN Diagnosis. First, the presence of symptoms is analysed. If symptoms are present in the time series from BMS data, the 'present' state will be sent as a time series input into the DBN model. Based on this input, the DBN delivers probable faults along with their occurrence probabilities, thereby offering building manager or maintenance teams insights in the operational faults. Conversely, if no symptoms are present, the corresponding fault probabilities are zero.

2.4 Posterior probability calculation

An arbitrary rule is applied for diagnosing faults based on their posterior probabilities:

- No fault is detected if the probability is below 50%.
- A fault is diagnosed if the probability exceeds 50%.

The Fault Diagnosis Efficiency (FDE) index measures diagnosis performance, particularly useful for time series data in BMS, as seen in various studies [16, 17, 19-21]. This index evaluates how often a fault is detected over a day. For instance, a single detection out of 144 ten-minute intervals suggests a random occurrence, whereas 80 detections indicate a consistent fault. The FDE index is calculated by dividing the number of detections over a severity threshold of 0.5 by the total number of checks in a day, reflecting the likelihood and assumption of a fault condition for a specific component, the index is expressed as:

$$FDE_j = \frac{1}{N}\sum_{i=1}^{N} I\left(f_{ij} > 0.5\right) \quad (3)$$

Where I is an indicator function that evaluates to 1 when the condition is true (i.e., the fault severity level f_{ij} for the j^{th} component in the i^{th} sample is greater than 0.5), *and* N is the number of samples.

3. Case study

To demonstrate the fault diagnostic capabilities of the 4S3F DBN, the experimental data from an office building (Kropman, Breda) in the Netherlands is used for evaluation. Specific faults were introduced at certain times, and the recorded BMS data was used to carry out the diagnostic. Fig. 3 shows the P&ID of the AHU with HRW in the building.

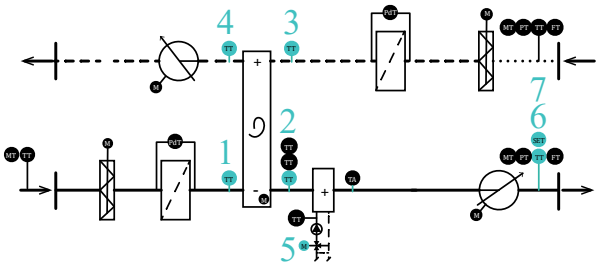

Fig. 3. P&ID of the AHU in the office building

The faulty data was collected during the period 12-02-2023 to 09-11-2023 . Seven sensors, with a data collection interval of one minute are used in this research. This AHU consists of several components, two fans (supply and return), two filters (supply and return), two dampers, heat recovery wheel, heating coil system. Sensors used in this research are temperature sensors (1,2,3,4,6) ,valve positions of heating coil system (5), and return air temperature from the rooms (7). The DBN is created to detect faults relating to the heat recovery wheel and the heating coil system.

3.1 Fault and symptom nodes

Table 1. introduces two fault nodes. It is assumed that most time there are no faults: the prior probability of fault F_1 not occurring is 0.9. For F_2 is 0.80. For a discussion about the impact of the prior probabilities on the results, see [17, 19-21].

Table 1. Fault nodes and prior probabilities

#	Fault	State	Prior Probability
F_1	Heating Coil Valve	Faulty	0.1
		Normal	0.9
F_2	Heat recovery wheel	Failure	0.05
		Stuck	0.15
		Normal	0.80

Table 2. Variable abbreviations

#	Name of variable	Abbreviation	Unit
1	Supply air temperature	T_{sa}	$°C$
2	Temperature after HRW	T_a	$°C$
3	Return air temperature	T_{ra}	$°C$
4	Outdoor air temperature	T_{oa}	$°C$
5	Set point temperature	T_{set}	$°C$
6	Heating coil valve openness	U_{hc}	%
7	Heat recovery wheel efficiency	η_{sup}	%

Table 3. Symptoms rules and definitions

#	Symptom	State	Rule of state definition
S_1	Difference of HCV position prediction	Present	$\lvert U_{hc} - U_{hc,\text{pred}}\rvert > \varepsilon_{hc}$
		Normal	$\lvert U_{hc} - U_{hc,pred}\rvert \leq \varepsilon_{hc}$
S_2	Difference of setpoint & supply temp	Present	$\lvert T_{set} - T_{sa}\rvert > \varepsilon_{ts}$
		Normal	$\lvert T_{set} - T_{sa}\rvert \leq \varepsilon_{ts}$
S_3	HCV openness frozen	Present	$\lvert U_{hc,max} - U_{hc,min}\rvert \leq \varepsilon_f$
		Normal	$\lvert U_{hc,max} - U_{hc,min}\rvert > \varepsilon_f$
S_4	HRW efficiency	Present	$\lvert \eta_{sup} - \eta_{design}\rvert > \varepsilon_{hrw}$
		Normal	$\lvert \eta_{sup} - \eta_{design}\rvert \leq \varepsilon_{hrw}$
S_5	Difference between temp before HRW and after	Present	$\lvert T_a - T_o\rvert \leq \varepsilon_t$
		Normal	$\lvert T_a - T_o\rvert > \varepsilon_t$

Fault Node 1 (F_1), heating coil valve position, represents a control fault indicating a malfunction within the control system that affects the heating coil valve's ability to open correctly, potentially impacting the heating system's overall performance.

Fault Node 2 (F_2), heat recovery wheel, has three states which covers two fault types:

- Failure ($F_2 - ST_1$): Represents a complete malfunction of the heat recovery wheel, where it ceases to rotate and to contribute to the heat exchange process. This is a component fault.

- Stuck ($F_2 - ST_2$): Indicates a scenario where the wheel is hindered from rotating at the right speed, potentially due to mechanical obstructions or system control faults, thus impairing its efficiency. This fault can be control or component.
- Normal: Denotes the condition where the heat recovery wheel is operating within its designed parameters, effectively rotating at the prescribed speed without any mechanical or control system impediments.

F_2 is designed to be a multi-state node, capable of discerning between a component failure, a control-related stuck condition, and a normal operating state. Table 2. and Table 3. describes variables involved in the symptom calculation, 5 symptoms are used in this research.

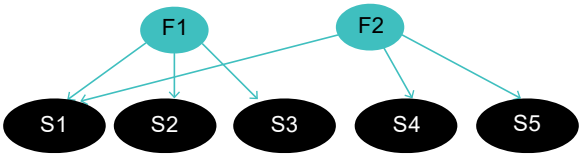

Fig. 4. DBN Structure

Symptom 1 (S_1), discrepancy in heating coil valve position, measures the deviation (ε_{hc}) of the actual valve position from the expected position as predicted by a AI algorithm called XGBoost (extreme gradient boosting) model, proposed by Chitakara [22]. This symptom is EP symptom and indicative of F_1 and is also a common symptom affecting F_2 in AHU with HRW since a stuck HRW result in higher openness of the valve. A labeled faulty and fault free data set is needed to use this symptom. The ε_{hc} is set to 3% in this case and it is obtained from expert knowledge.

Symptom 2 (S_2), difference in actual supply temperature (T_{sa}) and set point temperature (T_{set}), is an OS symptom. The presence of this symptom can be because of a wrong heating coil valve position (F_1). It is excluded that it comes from F_2, as the heating coil was designed to be able to deliver enough heat in Kropman office, even if the HRW is not working. The symptom present threshold ε_{ts} is derived from BMS specification and set to 2 in this case. The condition for observation of a symptom is given in Table 3**.**

Symptom 3 (S_3), heating coil valve openness frozen, presents itself when no variation(ε_f) is observed in the openness which could fix its openness in certain percentage, this impacts directly F_1 directly. This symptom is an OS symptom. The symptom detect threshold ε_f is set to 0.1 in this case and it is obtained from expert knowledge. The number of consecutive readings that must be frozen to trigger the valve frozen symptom is set to 5.

Symptom 4 (S_4), heat recovery wheel efficiency, presents itself when the difference between operational efficiency and designed efficiency of HRW is lower than the expected threshold (ε_{hrw}). The presence of S_4 could be symptomatic of either a failure or a stuck condition, which corresponds to two different states of F_2 . This symptom is EP symptom. The symptom detection threshold ε_{hrw} is set to 0.72, which was obtained from the HRW specification document and data analysis.

Symptom 5 (S_5): Temperature Difference Across Heat Recovery Wheel This symptom measures the temperature difference (ε_t) of supply air before and after the heat recovery wheel. Too low differences can be a failure or a stuck condition, linking to two different states of F_1. This symptom falls under the category of an Energy Performance (EP) symptom. The threshold, denoted as ε_t has been established at a value of 2. This threshold value is derived from theoretical principles of system thermal dynamics in conjunction with expert knowledge in the field.

Symptoms S_1, S_4, and S_5 are therefore associated with F_2providing a diagnostic indication of the wheel's operational status. Symptom S_1, despite its primary connection to the F_1, serves as a shared symptom due to its relevance in detecting discrepancies in system control, which can affect both the HCV and the HRW (e.g. if the heat recovery is not working properly, this could lead to compensation by the heating coil). Symptoms S_2 and S_3 are exclusively connected to F_1, providing diagnostics for the HCV position issues. Fig. 4**.** shows the structure of DBN with the above symptoms and faults.

3.2.2 Probabilities

In the DBN model, each fault node has several possible states. The occurrence of either of these states is an integral event, serving as critical evidence in the fault diagnosis process. Prior probabilities are assigned to each state. To further set up the DBN model, a CPT is used. This table articulates the probabilities of each state of a symptom node, considering all possible state combinations of its parent nodes. The CPT is vital in determining how fault node states affect the probability distribution of a symptoms node's states.

However, given the limited availability of detailed survey data on prior and especially conditional probabilities of faults in AHU systems, the estimation of these parameters has been assumed by the authors. This estimation is based on the authors' expertise, literature study [12, 16, 17, 23], first principles and interviews. For example, Table 4. shows a CPT of HRW states and efficiency symptom. If the HRW efficiency drops below the threshold, it is reasonable to assume that the possibility of the stuck fault should be a little bit higher (0.7) than the completely failure fault (0.6), since the HRW may still working this situation. Conversely, if the HRW efficiency symptom is present, the probability of HRW working normally should be relatively low (0.3). For a discussion about the impact of the conditional probabilities on the diagnostic, see [17]

Table 4. Conditional probability table of HRW

HRW State	P(Efficiency=0)	P(Efficiency=1)
Normal	0.9	0.1
Stuck	0.3	0.7
Failure	0.4	0.6

3.2.3 Data collection

The experimental phase involved the implementation of various fault conditions in the AHU system to assess the DBN's diagnostic proficiency. The Table 5. summarized the faults introduced during the experiments. Cases 1 through 4 pertain to the same fault implemented at different severity levels and serve to analyse the model's sensitivity to the detection of a fault at various 'stuck levels'.

4. Result and discussion

This section begins with a description of the establishment of symptom thresholds and an analysis of their impact on the accuracy of the Diagnostic Bayesian Network (DBN) model. This is followed by an interpretation of the diagnostic results for full DBN.

Table 5. Introduced faults

Case	Date	Time	Component	Induced Fault
1	08-03-2023	9:00-16:00	HRW	Stuck at 80% ($F_2 - ST_2$)
2	27-02-2023	9:00-16:00	HRW	Stuck at 50% ($F_2 - ST_2$)
3	09-11-2023	9:00-16:00	HRW	Stuck at 30% ($F_2 - ST_2$)
4	08-11-2023	9:00-16:00	HRW	Stuck at 10% ($F_2 - ST_2$)
5	22-03-2023	9:00-16:00	HRW	Failure ($F_2 - ST_1$)
6	28-02-2023	9:00-16:00	HCV	Stuck at 10/40/100% (F_1)
7	27-03-2023	9:00-16:00	HCV	Stuck at 75% (F_1)
8	02-02-2023	9:00-16:00	Normal	None

4.1 Analysis of symptoms and threshold

The number and types of symptoms, and the values of thresholds impact decisively the diagnostic results decisively. Fig. 5. illustrates the efficiency of the heat recovery wheel in case 1, 2 and 8. ε_{hrw} is also can obtained from HRW specifications when labelled data is unavailable. As described in the figure, the efficiency of the HRW on a normal day (Case 8) is around 0.73 and the efficiency of HRW stuck at 80% (Case 1) is between 0.69 to 0.72. The efficiency of the HRW stuck at 50% (Case2) is around 0.625 most of the time. This figure underscores clear efficiency boundaries between levels of symptoms, showing that lower rotation speed means lower efficiency. Therefore, in order to precisely distinguish the symptoms of nearly normal scenario like 80% rotation speed (Case1) from the normal scenario, the threshold should be set in between 0.72 to 0.73.

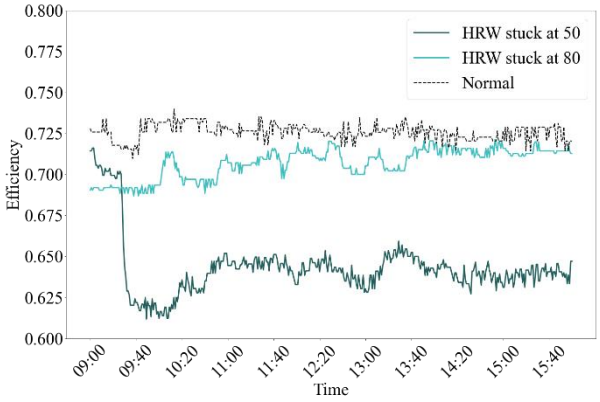

Fig. 5. HRW efficiency

Fig. 6. HCV prediction and actual position

In the DBN (Fig. 4.) model, S_1 is defined as a common symptom for F_1 and F_2, while these two faults also have two other symptoms (S_2 , S_3 and S_4 , S_5 respectively). This means that this model does not rely on single symptom to isolate fault. Fig. 6. shows Case 7's prediction and actual valve position. In order to test the advantage of multiple symptoms, S_1 has been manually removed from the measurement period. The result indicates that removing symptom S_1 from the dataset did not affect FDD, as demonstrate in Fig. 7.

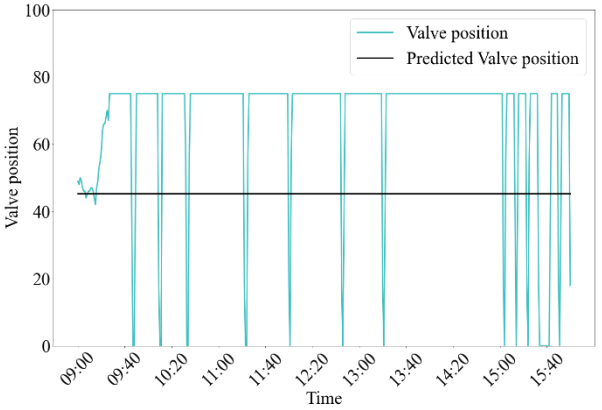

Symptoms S_1 and S_2 still precisely identified the fault F_1, confirming that multiple symptoms enhance FDD precision [17].

Among the five symptoms, the differential temperature before and after HRW denoted as S_5, specifically identifies HRW malfunctions or jams. Fig .8. showcases the impact of HRW speeds on temperature differences for cases 1, 2, 4, and 5, revealing that higher HRW speeds do not always lead to larger temperature changes; this may be due to varying outdoor temperatures or because HRW efficiency does not directly correspond to its speed. This symptom, an extension of S_4, indicates that with HRW inoperative, its efficiency drops to zero, leading to negligible temperature variance. This diagnostic symptom effectively pinpoints HRW issues, as demonstrated in Table 6.

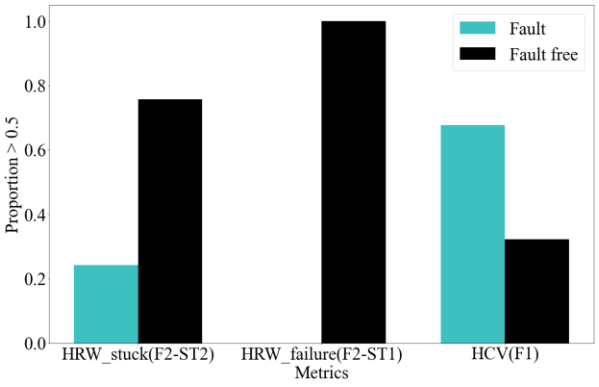

Fig. 7. Diagnosis result of case 7

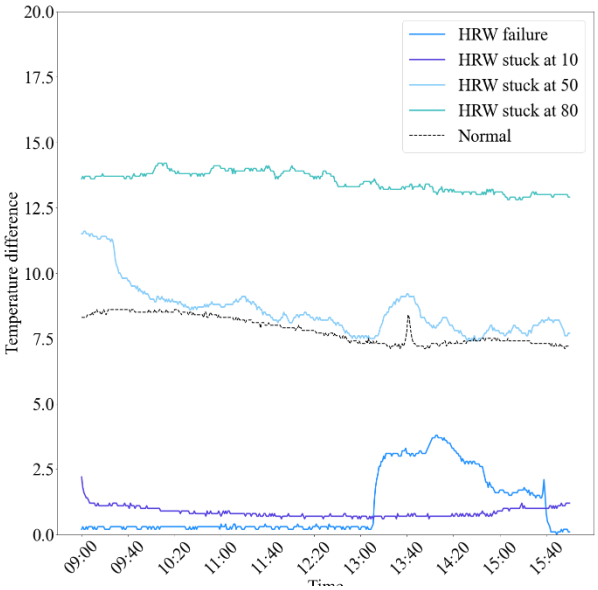

Fig. 8. Temperature difference before and after HRW

4.2 Analysis of diagnostic result

Table 6. shows the diagnostic result for each fault. The FDE index was calculated specifically for the period between 9:00 and 16:00, aligning with the scheduled working hours of the office on the days when faults were implemented. This approach was adopted to ensure that the FDE index accurately reflects the system's diagnostic performance under typical operating conditions. In Case 1, with the HRW nearly fully functional, tested the model's ability to differentiate between normal and near-normal conditions was tested, resulting in a high fault probability of around 0.99 for HRW stuck fault. In Case 2 and 3, where the HRW functioned at 50% and 30% respectively, the DBN accurately identified faults. Similarly, in Case 4, with the HRW stuck at a minimal operating condition of 10%, the FDE index consistently identified faults above a 0.5 probability threshold, highlighting the model's sensitivity to normal and nearly normal condition. In Case 5, a complete HRW failure was successfully diagnosed, underscoring the model's effectiveness in recognizing both control and component faults. Notably, in Case 5, the probability of F_1 exceeds the 0.5 threshold. This occurrence can be attributed to the HCV being nearly fully open (approximately 100% openness) as a compensatory mechanism for the heat that would typically be recovered by the Heat HRW. Despite this, it is observed that the failure of the HRW still registers the highest probability rate. Case 6 presented a more complex scenario with the HCV stuck at various positions (10%, 40%, 100%), where the DBN identified faults at each distinct position, exhibiting its capability to handle multifaceted fault conditions. Case 7, with the HCV at 0.67, posed a unique challenge due to its operation within a normal range but with performance deviations. Here, the FDD method accurately detected the nuanced fault condition. Finally, Case 8, representing a normal operation day without induced faults, served as a control scenario where the DBN maintained its diagnostic integrity by exhibiting probabilities below the fault threshold, thereby validating its accuracy and reliability in fault-free conditions.

Table 6. DBN diagnostic results

#	Fault	F_1	F_2		Isolated fault
		(HCV stuck)	ST_1 (HRW failure)	ST_2 (HRW stuck)	
1	HRW80%	0.00	0.00	0.99	$F_2 - ST_2$
2	HRW50%	0.00	0.00	0.89	$F_2 - ST_2$
3	HRW30%	0.20	0.00	0.76	$F_2 - ST_2$
4	HRW10%	0.00	0.00	0.67	$F_2 - ST_2$
5	HRW0	0.51	0.65	0.00	$F_2 - ST_1$
6	HCV 10/45/100 %	0.76	0.00	0.21	F_1
7	HCV 75%	0.67	0.00	0.24	F_1
8	Normal	0.00	0.00	0.00	none

5. Conclusion and discussion

This research has showcased the capability of DBN in accurately diagnosing faults in AHU components, specifically focusing on the HRW and HCV.

The study underscored the importance of setting accurate symptom thresholds for diagnosis. For example, adjusting the threshold and bandwidth for the S_3 affects its detection and the duration it is considered present. Higher thresholds decrease sensitivity for detecting a frozen valve, while bandwidth adjustments alter the frequency of S_3 present. These adjustments are crucial as they significantly influence the DBN's diagnostics, particularly for strongly correlated symptoms like S_3. The research also showed that even without some symptoms, like S_1, the system could reliably isolate F_1, This successful isolation can be attributed to the rich sensor environment integrated into the AHU emphasizing the benefit of incorporating multiple symptoms to improve diagnostic accuracy.

Furthermore, the research brought into focus how environmental factors like outdoor temperature can influence the symptoms, necessitating adaptable threshold settings following the rules of control used in the AHU.

In conclusion, this research establishes the DBN's ability to handle complex fault conditions and also contributes to increasing the knowledge on FDD of AHU heating systems' using HRW.

Future research should aim at exploring the level of details needed (i.e. for which applications should the DBN be able to diagnose levels of fault, and for which could it be binary) and at expanding the DBN's applicability in diverse AHU systems configurations, exploring the integration of additional sensors or virtual sensors. Investigating the impact of external factors like environmental conditions on system performance and fault diagnosis could also yield further insights.

Acknowledgement

This research was carried out as part of the Brains for Buildings project [18], sponsored by the Dutch grant program for Mission-Driven Research, Development and Innovation (MOOI). This program was established by the Dutch Ministry of Economic Affairs and Climate Change and the Ministry of the Interior and Kingdom Relations and executed by RVO Netherlands Enterprise Agency. The work is also supported by Kropman Installatietechniek. Special thanks to John Verlaan, and Shalika Walker at Kropman for facilitating the experiment.

References

1. Energy system, https://www.iea.org/energy-system
2. Pérez-Lombard, L., Ortiz, J., Pout, C.: A review on buildings energy consumption information. Energy Build. 40, 394–398 (2008).
3. Isermann, R.: Fault-Diagnosis Systems. Springer, Berlin, Heidelberg (2006)
4. Lin, G., Kramer, H., Granderson, J.: Building fault detection and diagnostics: Achieved savings, and methods to evaluate algorithm performance. Build. Environ. 168, (2020).
5. Zhao, Y., Li, T., Zhang, X., Zhang, C.: Artificial intelligence-based fault detection and diagnosis methods for building energy systems: Advantages, challenges and the future. Renew. Sustain. Energy Rev. 109, 85–101 (2019).
6. Rogers, A.P., Guo, F., Rasmussen, B.P.: A review of fault detection and diagnosis methods for residential air conditioning systems. Build. Environ. 161, (2019).
7. Zhao, Y., Zhang, C., Zhang, Y., Wang, Z., Li, J.: A review of data mining technologies in building energy systems: Load prediction, pattern identification, fault detection and diagnosis. Energy Built Environ. 1, 149–164 (2020).
8. Wu, B., Cai, W., Chen, H., Zhang, X.: A hybrid data-driven simultaneous fault diagnosis model for air handling units. Energy Build. 245, (2021).
9. Cheng, F., Cai, W., Zhang, X., Liao, H., Cui, C.: Fault detection and diagnosis for Air Handling Unit based on multiscale convolutional neural networks. Energy Build. 236, (2021).
10. Yan, R., Ma, Z., Kokogiannakis, G., Zhao, Y.: A sensor fault detection strategy for air handling units using cluster analysis. Autom. Constr. 70, 77–88 (2016).
11. Kim, W., Katipamula, S.: A review of fault detection and diagnostics methods for building systems. Sci. Technol. Built Environ. 24, 3–21 (2018).
12. Zhao, Y., Wen, J., Xiao, F., Yang, X., Wang, S.: Diagnostic Bayesian networks for diagnosing air handling units faults – part I: Faults in dampers, fans, filters and sensors. Appl. Therm. Eng. 111, 1272–1286 (2017).
13. Li, T., Zhou, Y., Zhao, Y., Zhang, C., Zhang, X.: A hierarchical object oriented Bayesian network-based fault diagnosis method for building energy systems. Appl. Energy. 306, (2022).
14. Wang, Z., Wang, Z., Gu, X., He, S., Yan, Z.: Feature selection based on Bayesian network for chiller fault diagnosis from the perspective of field applications. Appl. Therm. Eng. 129, 674–683 (2018).
15. Cai, B., Liu, Y., Fan, Q., Zhang, Y., Liu, Z., Yu, S., Ji, R.: Multi-source information fusion based fault diagnosis of ground-source heat pump using Bayesian network. Appl. Energy. 114, 1–9 (2014).
16. Dey, D., Dong, B.: A probabilistic approach to diagnose faults of air handling units in buildings. Energy Build. 130, 177–187 (2016).
17. Taal, A., Itard, L.: P&ID-based automated fault identification for energy performance diagnosis in HVAC systems: 4S3F method, development of DBN models and application to an ATES system. Energy Build. 224, (2020).
18. About – Brains4buildings, https://brains4buildings.org/about/
19. Taal, A., Itard, L.: P&ID-based symptom detection for automated energy performance diagnosis in HVAC systems. Autom. Constr. 119, (2020).
20. Taal, A., Itard, L., Zeiler, W.: A reference architecture for the integration of automated energy performance fault diagnosis into HVAC systems. Energy Build. 179, 144–155 (2018).
21. Taal, A., Itard, L.: Fault detection and diagnosis for indoor air quality in DCV systems: Application

of 4S3F method and effects of DBN probabilities. Build. Environ. 174, (2020).
22. Chitkara, S., van den Brink, A.H.T.M., Walker, S.S.W., Zeiler, W.: An early prototype for fault detection and diagnosis of Air-Handling Units. Proc. Clima 2022. 1–8 (2022)
23. Zhao, Y., Wen, J., Wang, S.: Diagnostic Bayesian networks for diagnosing air handling units faults – Part II: Faults in coils and sensors. Appl. Therm. Eng. 90, 145–157 (2015).